Petroleum Science 22 (2025) 4645–4655

Contents lists available at ScienceDirect

Petroleum Science

journal homepage: www.keaipublishing.com/en/journals/petroleum-science

Original Paper

Optimization and application of KCl polymer drilling fluid balancing wellbore stability and logging response accuracy

Xin Zhao [a,*], Ying-Bo Wang [b], Fu-Hua Cao [c,d], Cao-Yuan Niu [a], Zi-Qing Liu [b], Lei Wang [c]

[a] School of Petroleum Engineering, China University of Petroleum (East China), Qingdao, 266580, Shandong, China
[b] PetroChina Dagang Oilfield Company, Tianjin, 300280, China
[c] School of Geosciences, China University of Petroleum (East China), Qingdao, 266580, Shandong, China
[d] Logging Technology Research Institute, China National Logging Corporation, Xi'an, 710077, Shaanxi, China

ARTICLE INFO

Article history:
Received 10 April 2025
Received in revised form
14 October 2025
Accepted 14 October 2025
Available online 17 October 2025

Edited by Jia-Jia Fei

Keywords:
Induction logging
Logging interpretation accuracy
KCl concentration
Electrical resistivity
Wellbore stability
Water-based drilling fluid
Exploration/appraisal well

ABSTRACT

In Dagang Oilfield in China, the utilization of the KCl polymer water-based drilling fluid (WBDF) in mid-deep exploration/appraisal wells presents a challenge in simultaneously optimizing resistivity logging accuracy and wellbore stability. To address this, it is necessary to conduct geology-engineering integration studies. Based on the formation resistivity, an analytical model was developed to assess the impact of KCl concentration in the WBDF on array induction logging response accuracy. The maximum permissible KCl concentration for the target formations was determined, and technical strategies were proposed to maintain wellbore stability at a reduced KCl concentration. After that, considering the inhibitory, encapsulating, and plugging effects, a low-KCl-concentration WBDF was optimized and applied. Model calculations demonstrate that increasing KCl concentration in the WBDF decreases resistivity, thereby reducing logging accuracy. To maintain a logging accuracy of ≥80%, the upper limits for KCl concentration in the WBDF are 4.8%, 4.2%, and 3.6% for the 3rd Member of the Dongying Formation, the 1st and 2nd members of the Shahejie Formation, respectively. Cuttings recovery experiments revealed that a minimum KCl concentration of 3% is required to ensure basic shale inhibition. A combination of 3% KCl with 1% polyamine inhibitor yielded cuttings recovery and shale stability index comparable to those achieved with 7% KCl alone, and the shale inhibition performance was further enhanced with the addition of an encapsulator. The optimized WBDF has been successfully deployed in exploration/appraisal wells across multiple blocks within Dagang Oilfield, resulting in superior wellbore stability during operations. Furthermore, the electric logging interpretation coincidence rate improved from 68.1% to 89.9%, providing robust technical support for high-quality drilling and accurate reservoir evaluation in exploration/appraisal wells.

1. Introduction

In the Dagang Oilfield in China, exploration/appraisal wells exceeding 3500 m in depth predominantly employ the KCl polymer water-based drilling fluid (WBDF). While these fluids effectively mitigate clay shale hydration and promote wellbore stability, their typical KCl content (6%–7%) substantially decreases the drilling fluid's resistivity. This reduction is particularly pronounced in deep, high-temperature environments, significantly compromising the accuracy of array induction logging. Consequently, array curves exhibit notable separation, diminishing the ability to distinguish between oil and water-bearing strata. The influence of mineralization, specifically salt concentration, in drilling fluids on logging performance remains incompletely understood, and the critical mineralization threshold suitable for the target formations is yet to be definitely established. Attempts to enhance logging accuracy by reducing KCl concentration to 2%–4% in two wells resulted in a higher frequency of wellbore collapse and tripping-related incidents. Therefore, an urgent need exists to resolve the inherent conflict between logging interpretation accuracy and wellbore stability encountered in exploration/appraisal wells within this region when using KCl polymer drilling fluids.

* Corresponding author.
E-mail address: zhaoxin@upc.edu.cn (X. Zhao).
Peer review under the responsibility of China University of Petroleum (Beijing).

https://doi.org/10.1016/j.petsci.2025.10.012

The influence of drilling fluids on logging performance is governed by factors such as mineralization, filter cake thickness, soaking duration, and density (Zheng et al., 2014; Rasouli, 2022; Ramadan et al., 2024; Liu et al., 2025). In electrical logging, excessively high mineralization of the drilling fluid results in low resistivity and high conductivity, which reduces the apparent resistivity of hydrocarbon-bearing formations, increases the contribution from the borehole, and complicates the differentiation between oil and water-bearing zones. Furthermore, prolonged soaking of the drilling fluid extends its invasion depth, progressively decreasing formation resistivity (Doughty et al., 2017; Lu et al., 2017; Li et al., 2019). Empirical evidence indicates that when the ratio of formation resistivity to drilling fluid resistivity is low, the amplitude variations of induction logging curves correspond to formation characteristics, and the spontaneous potential curve is clearly defined. Conversely, when this ratio is excessively high, the deep-reading induction curve, which primarily reflects the original formation resistivity, is less affected, while the shallow-reading curve exhibits anomalous separation due to the borehole effects. Concurrently, the amplitude of the positive anomaly in the spontaneous potential curve is attenuated, rendering it less effective for formation delineation (Jiang et al., 2021; Baggieri et al., 2024; Sukhorukova et al., 2025). With respect to nuclear magnetic resonance (NMR) logging, low drilling fluid resistivity intensifies antenna negative feedback, diminishes NMR logging gain, impairs instrument operational stability, and exacerbates signal attenuation (Xu et al., 2013; Kozlowski et al., 2021). Consequently, logging service companies have established a lower limit for drilling fluid resistivity suitable for NMR logging instrumentation. Therefore, in the context of exploration/appraisal wells within the Dagang Oilfield, controlling the KCl concentration within the drilling fluid is crucial for adjusting drilling fluid resistivity, and, by extension, the concentration of conductive ions, to ensure accurate array induction logging responses. This control is essential for obtaining clear and reliable spontaneous potential and induction resistivity curves, facilitating the calculation of original formation oil saturation and enabling effective discrimination between oil and water-bearing intervals (Zhao et al., 2023; Wang et al., 2024). However, excessively low KCl concentrations may compromise the drilling fluid's capacity to mitigate wellbore instability (Shi et al., 2019).

To address the aforementioned challenges, it is imperative to analyze the influence of KCl concentration in the drilling fluid on logging accuracy, accounting for the specific characteristics of the target formations in exploration/appraisal wells within the Dagang Oilfield. This analysis will facilitate the determination of the maximum permissible KCl concentration or mineralization level in the drilling fluid necessary to ensure accurate logging of the target formations. Furthermore, the investigation of drilling fluid technologies capable of effectively maintaining clay shale wellbore stability within the KCl concentration range required for logging accuracy is essential. The objective of this research is to optimize a high-performance wellbore-stabilizing drilling fluid system, thereby simultaneously ensuring robust wellbore stability and reliable logging interpretation.

2. Analysis of the impact of drilling fluid KCl concentration on array induction logging

2.1. Geology settings of Dagang Oilfield

The typical geology settings of Dagang Oilfield are shown in Table 1. In the present work, the target formations include the 3rd Member of the Dongying Formation (Dong-3 Member), the 1st Member of the Shahejie Formation (Sha-1 Member), and the 2nd Member of the Shahejie Formation (Sha-2 Member).

2.2. Modeling and data processing for induction logging

Based on resistivity data from 12 wells within the Dagang Oilfield, the target formations exhibit the following characteristics: the resistivity of the Dong-3 Member ranges primarily from 1.3 to 19.7 Ω·m, with a mean resistivity of 3.5 Ω·m. The Sha-1 Member exhibits a resistivity range of 1.9–20.4 Ω·m, with an average resistivity of 4.5 Ω·m. The Sha-2 Member displays resistivity values ranging from 4.6 to 21.7 Ω·m, with a mean resistivity of 10 Ω·m.

To investigate the influence of various drilling fluid types (saltwater, freshwater, and oil-based) on array induction logging response accuracy across a spectrum of formation resistivities (ranging from low to high), a model of a homogeneous and isotropic formation was developed, as depicted in Fig. 1.

Accounting for the KCl concentration and resistivity range of the drilling fluid, as well as the formation resistivity of the target block, models were developed with varying KCl mass-volume concentrations for the Dong-3 Member (120 °C), Sha-1 Member (135 °C), and Sha-2 Member (150 °C). Analysis of logging data from drilled wells reveals that the raw formation conductivity signals acquired by the array induction logging instrument are influenced by factors such as borehole size, drilling fluid invasion, and the skin effect, thereby precluding direct representation of the in-situ formation properties (Yang et al., 2023; Xiong et al., 2024). Consequently, the sequential application of skin effect correction, borehole correction, and focusing synthesis processing to the raw data is necessary to mitigate or eliminate the influence of these factors and derive the true formation conductivity.

Table 1
Geology settings of Dagang Oilfield.

Formation	Subunit	Thickness, m	Lithology description
Minghuazhen Formation	/	1000–1600	Upper part: interbedded light brown mudstone and brown-yellow sandstone Lower part: brown-red or dark red mudstone with green-gray and light gray sandstone
Guantao Formation	/	300–400	Gray-white sandstone, pebbly sandstone interbedded with purple-red and gray-green mudstone
Dongying Formation	Dong-1 Member	0–700	Gray sandstone and gray-green mudstone
	Dong-2 Member	100–300	Gray and green-gray mudstone interbedded with sandstone
	Dong-3 Member	> 100	Mudstone and gray sandy mudstone interbeds
Shahejie Formation	Upper Sha-1 Member	> 100	Gray mudstone with sandstone layers
	Middle Sha-1 Member	> 100	Dominantly dark gray mudstone and shale, with gray siltstone interbeds
	Lower Sha-1 Member	50–400	Oil shale and dark sandy mudstone interbeds
	Sha-2 Member	0–400	Gray-green and gray mudstone interbedded with light gray sandstone
	Sha-3 Member	400–1000	Frequent interbeds of conglomerate and mudstone, with thick dark mudstone layers and grouped sandstone/conglomerate intercalations

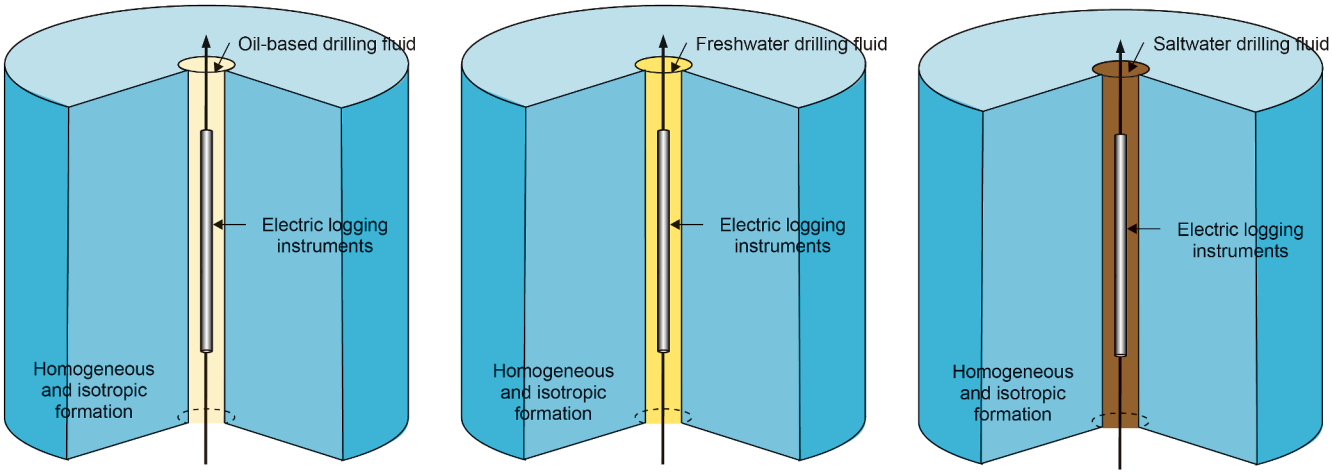

Fig. 1. Schematic diagram of a homogeneous and isotropic formation model.

Using the HDIL (high definition induction logging) array induction logging instrument as an illustrative example, the raw measurement data comprise the real and imaginary components of 7 sub-arrays and 8 frequencies (10, 30, 50, 70, 90, 110, 130, and 150 kHz), yielding a total of 112 logging curves. The processing workflow primarily includes the following three stages: (1) Skin effect correction: To enhance the accuracy of conductivity measurements in heterogeneous formations, the instrument response and the linear relationship between the instrument and formation conductivity were improved. Following depth resampling of the 56 pertinent curves, skin effect correction was initially performed. (2) Borehole effect correction: Typically, geometric factor correction or adaptive correction methods were employed to eliminate measurement errors arising from borehole factors. (3) Standard synthesis focusing processing: Curves characterized by varying resolutions and detection depths were processed utilizing digital filtering to generate synthetic signals with fixed resolution and varying detection depths, thereby improving the resolution of the raw measurement signals and unifying the response characteristics of signals at different detection depths.

2.3. Array induction logging response analysis

2.3.1. Synthetic logging response curves for different formations

To facilitate a comprehensive analysis of the influence of drilling fluid resistivity on logging response, a homogeneous, isotropic formation model was utilized, maintaining a constant borehole diameter of 8 inches and varying the drilling fluid resistivity from 0.01 to 100 Ω·m. Formation resistivity values for the Dong-3 Member, Sha-1 Member, and Sha-2 Member were set at 3.5, 4.5, and 10 Ω·m, respectively. Simulation calculations were then performed to generate array induction logging response curves for the three formations at different drilling fluid resistivities, as illustrated in Fig. 2.

The synthetic logging response curves presented are the result of two-inch resolution matching across various spacings (10, 20, 30, 60, 90, and 120 inches). Observations reveal that logging curves corresponding to different source-receiver spacings exhibit varying sensitivities to drilling fluid resistivity, with short-spacing curves being more susceptible and long-spacing curves being less affected. Under consistent formation resistivity conditions, the influence of drilling fluid resistivity on the array induction logging response diminishes as drilling fluid resistivity increases, leading to curve convergence and approximation of the true formation resistivity value. In practice, the 10-inch curve is typically excluded due to its significant susceptibility to borehole effects. The 60-inch, 90-inch, and 120-inch curves generally exhibit applicability across a range of drilling fluid conditions. Consequently, the primary focus is directed towards investigating the impact of drilling fluid on the 20-inch and 30-inch curves to establish the upper limit of KCl concentration or salinity in the drilling fluid that ensures accurate well logging within the target formation.

2.3.2. The impact of KCl drilling fluid resistivity on logging response accuracy

Based on the results presented in Fig. 2, the logging response accuracy of the 20-inch and 30-inch curves under varying drilling fluid resistivity conditions was analyzed, as depicted in Fig. 3. Logging response accuracy is defined as the ratio of the corrected logging data to the true formation resistivity. Across the three distinct formations, the accuracy of the logging curves exhibits an inverse relationship with drilling fluid resistivity. From a logging performance perspective, the critical drilling fluid resistivity threshold required to maintain a response accuracy of at least 80% is determined by the formation resistivity. For the Dong-3 Member (Fig. 3(a)), where the formation resistivity predominantly approximates 3.5 Ω·m, a downhole drilling fluid resistivity exceeding 0.018 Ω·m ensures a measurement accuracy for the 20-inch and 30-inch curves surpassing 80%, thereby satisfying the requirements for electrical logging curve accuracy. Similarly, for the Sha-1 Member (Fig. 3(b)), characterized by a formation resistivity primarily around 4.5 Ω·m, a downhole drilling fluid resistivity above 0.021 Ω·m guarantees a measurement accuracy for both curves exceeding 80%. For the Sha-2 Member (Fig. 3(c)), where the formation resistivity predominantly measures approximately 10 Ω·m, a downhole drilling fluid resistivity greater than 0.043 Ω·m is necessary to meet the logging curve accuracy criteria.

2.3.3. The impact of drilling fluid KCl concentration on logging accuracy

Based on the computational results presented in Fig. 3, and considering the resistivity of KCl aqueous solutions at varying mass-volume concentrations under surface temperature conditions (18 °C), along with the conversion relationship between formation temperature and downhole drilling fluid resistivity at surface temperature, the salinity, or salt concentration, of the drilling fluid in formations at different temperatures was calculated. Subsequently, the influence of drilling fluid salt

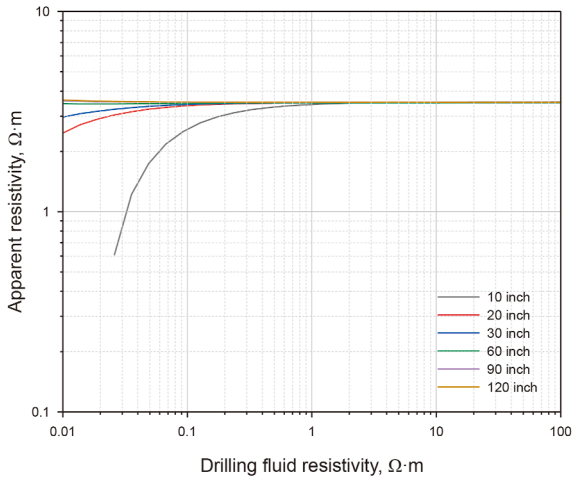

(a) Dong-3 Member

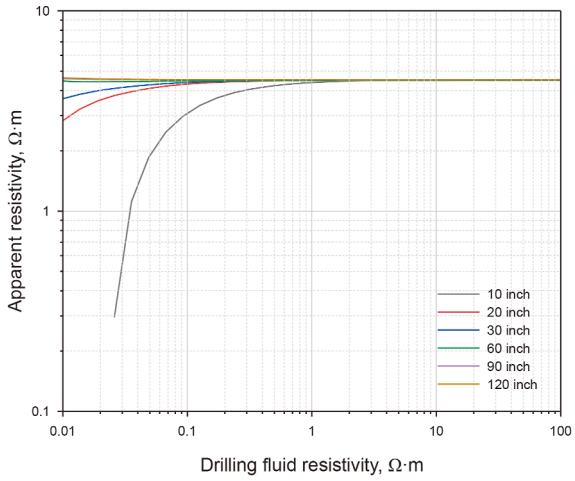

(b) Sha-1 Member

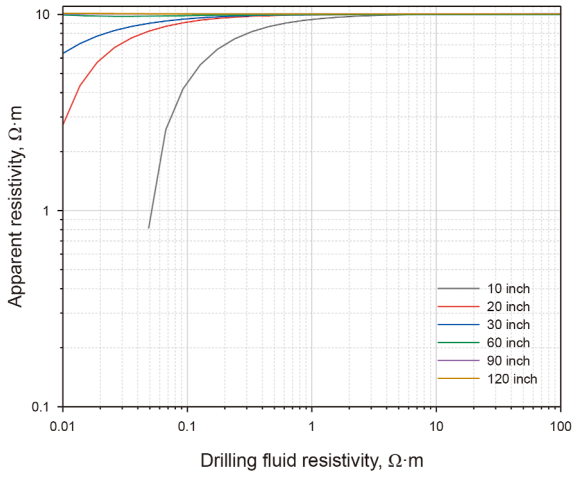

(c) Sha-2 Member

Fig. 2. Composite diagram of logging response for different formations.

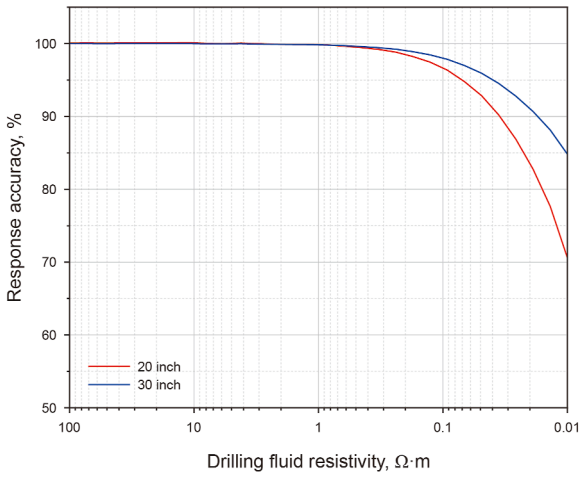

(a) Dong-3 Member

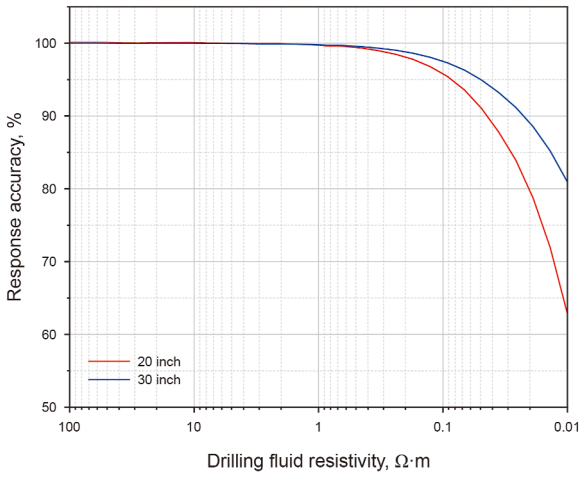

(b) Sha-1 Member

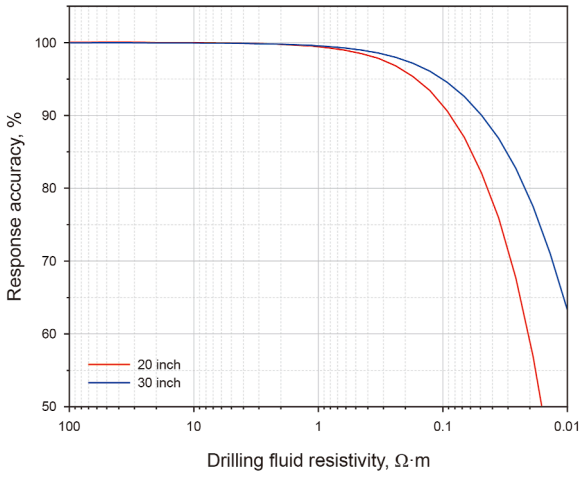

(c) Sha-2 Member

Fig. 3. Logging response accuracy maps for different formations.

concentration on logging accuracy was analyzed, with the results illustrated in Fig. 4.

The data indicate that as the salt concentration of the drilling fluid increases, resistivity decreases, and the accuracy of the logging response curve declines. For the Dong-3 Member, characterized by a formation temperature of 120 °C and a resistivity ranging from 1.3 to 19.7 Ω·m, maintaining the KCl concentration in the drilling fluid at $\leq$ 4.8% ensures that the logging accuracy for all

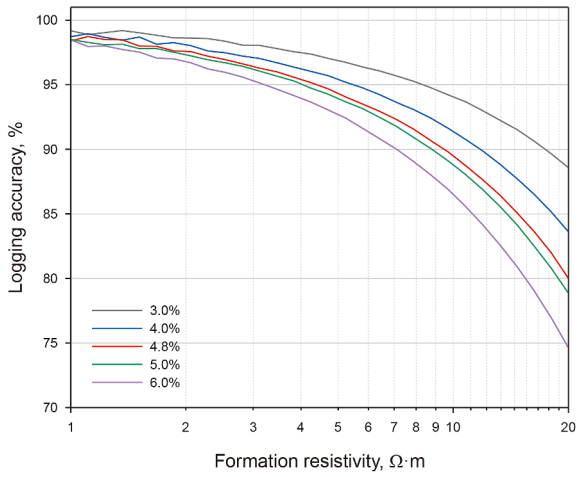

(a) Dong-3 Member

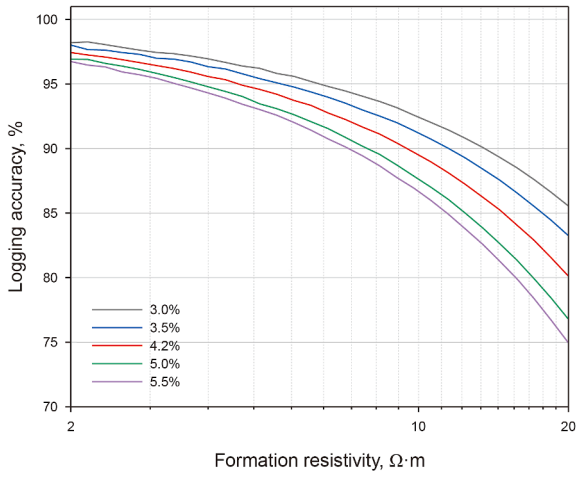

(b) Sha-1 Member

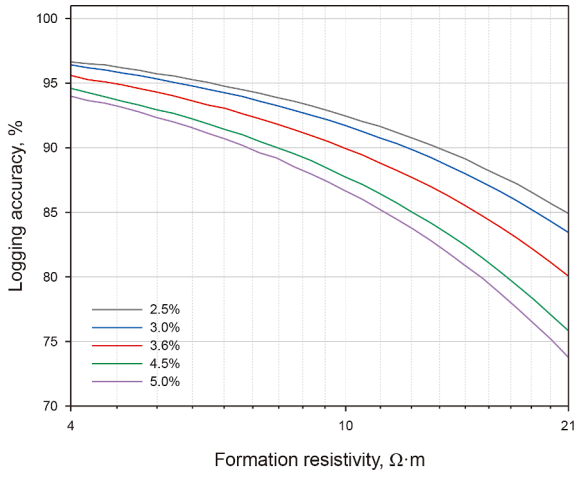

(c) Sha-2 Member

Fig. 4. Variations of logging response accuracy with the concentration of KCl in the drilling fluid.

formations within the Dong-3 Member reaches or exceeds 80%. Similarly, for the Sha-1 Member, with a temperature of 135 °C and a resistivity ranging from 1.9 to 20.4 Ω·m, a KCl concentration of ≤ 4.2% guarantees a logging accuracy of ≥ 80% for this formation. For the Sha-2 Member, which exhibits a temperature of 150 °C and a resistivity ranging from 4.6 to 21.7 Ω·m, the higher formation temperature necessitates a KCl concentration of ≤ 3.6% to counteract the decrease in drilling fluid resistivity and ensure a logging accuracy of ≥ 80% for this formation.

In summary, to ensure adequate logging accuracy across different formations, it is crucial to judiciously control the KCl concentration in the drilling fluid during drilling operations. This control is particularly important in the deeper Sha-2 Member with higher temperatures, where maintaining the KCl concentration at ≤ 3.6% is paramount.

3. Optimization of an effective wellbore-stabilizing drilling fluid at low KCl concentrations

Based on the analysis presented in Section 2.3.3, maintaining adequate logging accuracy necessitates controlling the KCl concentration to within 3.6%. However, in drilling operations within this area, the WBDF previously employed to ensure wellbore stability in shale formations contained a KCl concentration of 6%–7%. Reducing the KCl concentration, therefore, compromises the shale inhibition properties of the drilling fluid, increasing the risk of wellbore instability (Li et al., 2023; Murtaza et al., 2023; Xie et al., 2024). Consequently, the selection of effective non-electrolyte shale inhibitors that function synergistically with KCl, informed by the target formation's mineralogical composition, is crucial to maintaining adequate shale inhibition while reducing the KCl concentration.

3.1. Analysis of the mineralogical composition of the formation

Shale cuttings from a well within the Chenghai Block of Dagang Oilfield were selected for mineralogical analysis to characterize the composition of the target formation. The results are presented in Tables 2 and 3. The analysis reveals that the shale cuttings from the Dong-3 Member are predominantly composed of quartz, with clay minerals constituting 15.15%. Specifically, the illite/smectite (I/S) mixed-layer content is relatively high, accounting for 64% of the clay mineral fraction. The shale cuttings from the Sha-1 Member consist primarily of calcite and quartz, with clay minerals comprising 25.89%–27.95%. The I/S mixed-layer content in this member reaches 70% of the clay fraction. The shale cuttings from the Sha-2 Member are mainly composed of quartz, with a clay content of 28.37%, of which the I/S mixed-layer content accounts for 60%. These findings indicate that the rocks in the Shahejie Formation possess a relatively high clay mineral content, with abundant expansive I/S mixed-layer minerals. This mineralogical composition suggests a significant potential for hydration, swelling, and dispersion, rendering the formation susceptible to wellbore instability and operational challenges such as differential sticking during tripping operations.

3.2. Formulation optimization of an effective wellbore-stabilizing drilling fluid

3.2.1. Drilling fluid formulation optimization approach

The optimization approach, informed by the characteristics of the target formation and the multi-faceted, collaborative wellbore stability technology for drilling fluids (Zhang et al., 2019), prioritizes enhancing the plugging performance of the drilling fluid to minimize filtrate invasion into the formation. Following an assessment of the effect of KCl concentration on shale hydration inhibition within the target formation, an effective non-electrolyte shale inhibitor is selected for synergistic application with low-concentration KCl to effectively suppress shale hydration. Based

Table 2
Mineralogical content of shale cuttings.

Sample	Depth, m	Quartz, %	Potassium feldspar, %	Plagioclase, %	Calcite, %	Dolomite, %	Ankerite, %	Clay minerals, %
Dong-3 Member	2648	51.87	11.56	9.58	6.07	5.77	–	15.15
Sha-1 Member	2930	17.36	2.72	6.77	36.24	3.75	–	25.89
	3087	22.49	2.11	4.87	32.22	4.82		27.95
Sha-2 Member	3522	45.21	3.03	7.57	6.51	–	7.85	28.37

Table 3
Clay mineralogical content of shale cuttings.

Sample	Depth, m	Kaolinite, %	Chlorite, %	Illite, %	I/S mixed layers, %	Interlayer ratio, %
Dong-3 Member	2648	15	10	11	64	50
Sha-1 Member	2930	11	5	14	70	45
	3087	10	7	13	70	50
Sha-2 Member	3522	9	7	24	60	5

on the current application status of drilling fluid shale inhibitors and the research team's prior investigations, a low-molecular-weight polyamine was selected for combined use with KCl as shale inhibitors. The concentrations of these components employed in combination were optimized through experimentation, followed by the further selection of the high-efficiency encapsulator and plugging agent to refine the wellbore-stabilizing drilling fluid formulation.

3.2.2. Shale cuttings recovery rate test with different concentrations of KCl

Given the relatively low clay mineral content in the Dong-3 Member of the target block and the correspondingly high upper limit of KCl concentration (4.8%) permissible for maintaining logging accuracy in this formation, this study primarily focuses on the Sha-1 and Sha-2 members. Experiments on the shale cuttings recovery rate were widely used to evaluate the inhibition of drilling fluid on the dispersion of shales (Huang et al., 2021a; Sun et al., 2022). Rock samples obtained from the Sha-1 Member at depths of 2930 and 3087 m, and from the Sha-2 Member at a depth of 3522 m within a well in the Chenghai Block, were subjected to experimental evaluation of their recovery rate following rolling at 130 °C for 16 h in KCl solutions of different concentrations. The results are illustrated in Fig. 5. The rock sample from the Sha-1 Member at 2930 m exhibits a clay mineral content of 25.89%, primarily composed of illite-smectite mixed layers, which demonstrate significant hydration capacity. Consequently, its recovery rate in pure water is only 15.7%. Upon the addition of 3% KCl, the recovery rate increases to 46.9%, indicating that the addition of KCl effectively inhibits clay hydration. Further increases in KCl concentration result in a gradual increase in the recovery rate, albeit with a diminishing rate of increase. The recovery rates of the cuttings in 5% and 7% KCl solutions are 53.2% and 55.8%, respectively. Specifically, increasing the KCl concentration from 0% to 3% results in a 31.2% increase in the cuttings recovery rate, whereas subsequent increases to 5% and 7% improve the cuttings recovery rates by only 6.3% and 8.9%, respectively. The recovery rate variation patterns observed for the rock samples at 3087 and 3522 m in KCl solutions are consistent with those of the 2930 m rock sample. As the KCl concentration increases, the recovery rate gradually increases, with the rate of increase slowing down once the concentration exceeds 3%. Therefore, for the Sha-1 and Sha-2 members in this block, the KCl concentration in the drilling fluid should be maintained at a minimum of 3%. However, to ensure logging accuracy, the KCl concentration in the drilling fluid for the Sha-1 and Sha-2 members should be controlled within 4.2% and 3.6%, respectively. Thus, in field operations, the KCl concentration should be controlled within the range of 3%–4%. At this concentration level, formulation with high-efficiency shale inhibitors is required to guarantee optimal shale inhibition performance of the drilling fluid.

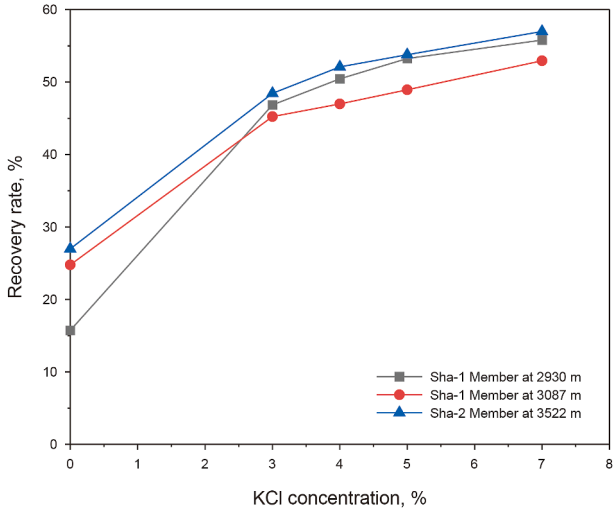

Fig. 5. Test results of cuttings recovery rate in KCl solutions.

3.2.3. Optimization of the blending ratio of KCl and polyamine

Analyzing the effect on clay interlayer spacing provides a direct method for assessing the polyamine's inhibition of clay hydration from a microscopic perspective. The molecular structure of the polyamine is shown in Fig. 6. Through X-ray diffraction analysis, the influence of different polyamine concentrations on the interlayer spacing of both dry and wet sodium bentonite samples can be determined, thereby characterizing its inhibition of clay hydration at the microscale. As illustrated in Fig. 7, for the dry samples, increasing the polyamine concentration to 0.5% results in an increase in the sodium bentonite interlayer spacing from 1.21 to 1.38 nm, indicating the intercalation of polyamine molecules into the interlayers of the sodium bentonite. Subsequently, further increases in the polyamine concentration do not induce any further changes in the interlayer spacing. This observation suggests that polyamine adsorbs as a monolayer between the clay layers. For the wet samples, increasing the polyamine concentration to 0.5% results in a decrease in the sodium bentonite interlayer spacing from 2.01 to 1.44 nm. As the polyamine concentration

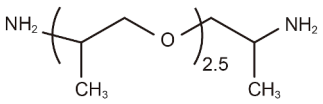

Fig. 6. Schematic diagram of polyamine molecular structure.

increases further, the interlayer spacing decreases slightly before stabilizing at 1.41 nm, demonstrating that polyamine effectively inhibits clay hydration even at low concentrations. Based on the molecular structure characteristics of polyamine (Zhong et al., 2011; Xie et al., 2024), the primary mechanism underlying its inhibition of clay hydration is as follows. Polyamine undergoes partial dissociation in aqueous solution to form ammonium cations, which neutralize the negative charges present on the surface of the clay, reducing the hydration repulsion of the clay. In addition, polyamine molecules can form hydrogen bonds with the surface of the clay crystal layers. The combined effect of electrostatic attraction and hydrogen bonding binds the clay layers together and expels a portion of the interlayer adsorbed water. Furthermore, the adsorption of polyamine on the clay surface enhances its hydrophobicity, preventing water molecules from entering the clay interlayers and further inhibiting clay hydration.

Having confirmed the suitability of polyamine as a non-electrolyte shale inhibitor, further evaluation was conducted to optimize its dosage and assess the shale inhibition performance of polyamine in combination with low-concentration KCl. The objective was to ensure that the shale inhibition effect was maintained despite the reduction of KCl concentration in the drilling fluid from 7% to 3%.

(1) Cuttings recovery experiment

Cuttings recovery experiments were performed on the Sha-1 and Sha-2 members to comparatively analyze the shale dispersion inhibition effect of the polyamine and 3% KCl combination against that of high-concentration KCl. Additionally, the improvement in inhibition performance resulting from the addition of an encapsulator named BYJ, which is a high-molecular-weight acrylamide-based polymer, was also analyzed. The results are presented in Fig. 8. The additives incorporated into each test sample are shown in Table 4.

The results indicate that, for the rock samples from the Sha-1 Member, the addition of 5% KCl and 7% KCl solutions resulted in an increase in the recovery rate from 24.8% to 48.9% and 52.9%, respectively, compared to pure water. The combination of 3% KCl with 1% polyamine yielded a cuttings recovery rate of 48.6%, comparable to that achieved with 5% KCl. Increasing the polyamine concentration to 2% further enhanced the recovery rate to 60.8%, surpassing the performance of 7% KCl. For the rock samples from the Sha-2 Member, the combination of 3% KCl with 1% polyamine resulted in a cuttings recovery rate of 59.3%, exceeding that obtained with 5% KCl (53.8%) and 7% KCl (57%). Further increasing the polyamine concentration to 2% led to a further improvement in the recovery rate to 62.8%. These findings suggest that the shale dispersion inhibition effect of 3% KCl combined with 1% polyamine is comparable to that of 5% KCl, while the combination of 3% KCl with 2% polyamine exhibits superior inhibition compared to 7% KCl. Further investigations were conducted to evaluate the effect of adding the encapsulator BYJ on the shale cuttings recovery rate. For the rock samples from the Sha-1 Member, the incorporation of 0.3% BYJ in combination with varying concentrations of KCl resulted in a further increase in the recovery rate. Specifically, the combination of 7% KCl with 0.3% BYJ yielded a recovery rate of 86.7%, demonstrating strong inhibition of shale hydration and dispersion. The recovery rate achieved with "3% KCl + 1% polyamine + 0.3% BYJ" reached 83.8%, also exhibiting excellent inhibition, and closely approaching the effect of "7% KCl + 0.3% BYJ". Increasing the polyamine concentration to 2% further improved the recovery rate to 85.4%. For the rock samples from the Sha-2 Member, the "3% KCl + 1% polyamine + 0.3% BYJ" combination resulted in a recovery rate of 76.8%, comparable to the inhibition effect observed with "7% KCl + 0.3% BYJ", which exhibited a recovery rate of 74.8%. However, increasing the polyamine concentration to 2% did not result in a significant improvement in the inhibition effect. Therefore, from the perspective of inhibiting shale hydration and dispersion, the effect of the combination of 3% KCl and 1% polyamine is comparable to that of 5%–7% KCl.

(2) Shale stability index experiment

The shale stability index (SSI) experimental method serves to reflect the comprehensive impact of changes in rock strength, swelling, and dispersion erosion under the influence of drilling fluids on wellbore stability. The SSI is calculated using the following formula (Mondshine, 1973):

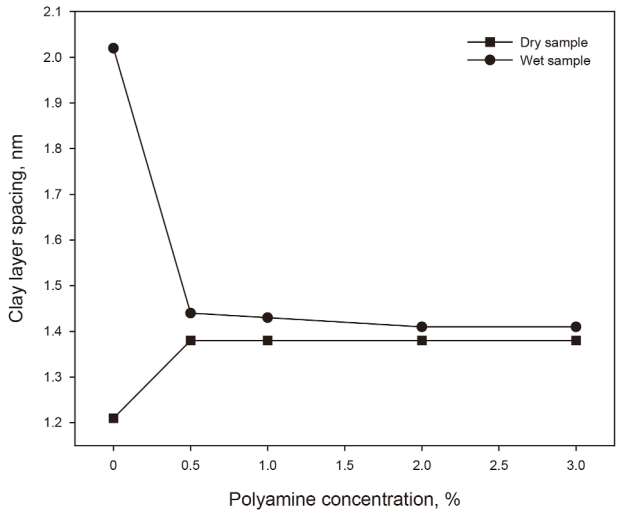

Fig. 7. Relationship between clay interlayer spacing and polyamine concentration.

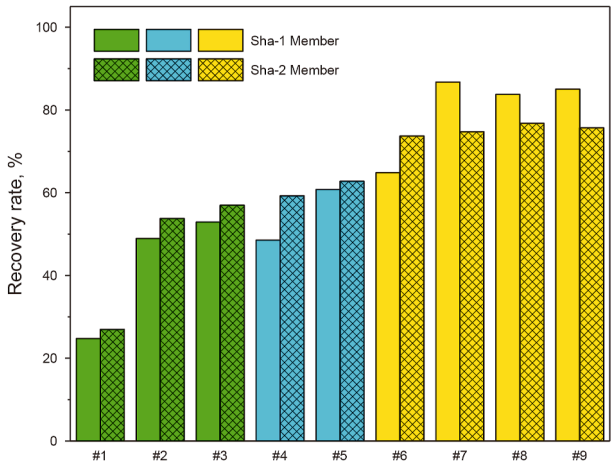

Fig. 8. Shale cuttings recovery rates in different inhibitor solutions.

Table 4
Additives incorporated into each test sample.

Sample No.	Additive concentration, %		
	KCl	Polyamine	BYJ
#1	0	0	0
#2	5	0	0
#3	7	0	0
#4	3	1	0
#5	3	2	0
#6	5	0	0.3
#7	7	0	0.3
#8	3	1	0.3
#9	3	2	0.3

$$SSI = 100 - 2\left(H_f - H_i\right) - 4D \quad (1)$$

where H_i is the penetration value of the rock sample prior to soaking, mm; H_f represents the penetration value of the rock sample after soaking, mm; D is the average swelling height or erosion depth of the rock sample after soaking in the drilling fluid, mm.

Using a rock sample from the Sha-1 Member, the SSI experiment was conducted to compare the shale stability effect of 3% KCl combined with polyamine to that of high-concentration KCl. The additives added into each test sample are shown in Table 5. The experimental results are presented in Fig. 9.

Under ideal conditions, where the rock sample does not undergo any hydration in the drilling fluid, for example, an excellent oil-based drilling fluid, the SSI value would be 100 (Mondshine, 1973). However, in practice, drilling fluids cannot completely prevent clay hydration. Following soaking in different solutions, lower SSI values indicate a higher degree of rock sample hydration, more severe degradation of rock strength, and poorer wellbore stability. Soaking the rock sample in pure water (Sample #1) resulted in an SSI value of only 15.9. Following soaking in KCl solutions (Samples #2 to #4), the SSI increased with increasing KCl concentration. The SSI values of the rock samples in 3% KCl, 5% KCl, and 7% KCl solutions were 45.8, 48.9, and 52.6, respectively, demonstrating that KCl significantly inhibited clay hydration, attenuated rock strength degradation caused by clay hydration, and facilitated improved wellbore stability in shale formations. The use of 3% KCl in combination with 1% and 2% polyamine yielded SSI values of 55.5 (Sample #5) and 61.8 (Sample #6), respectively. This indicates that the shale stability effect of 3% KCl combined with 1% polyamine was marginally superior to that of 7% KCl, and increasing the polyamine concentration further enhanced the wellbore-stabilizing effect. The combination of 7% KCl and "3% KCl + 1% polyamine" with 0.3% encapsulator BYJ resulted in SSI values of 73.1 (Sample #7) and 77.5 (Sample #8), respectively. This suggests that the incorporation of polymer encapsulators with shale hydration inhibitors further improves wellbore-stabilizing performance.

Table 5
Additives incorporated into each sample for SSI experiments.

Sample No.	Additive concentration, %		
	KCl	Polyamine	BYJ
#1	0	0	0
#2	3	0	0
#3	5	0	0
#4	7	0	0
#5	3	1	0
#6	3	2	0
#7	7	0	0.3
#8	3	1	0.3

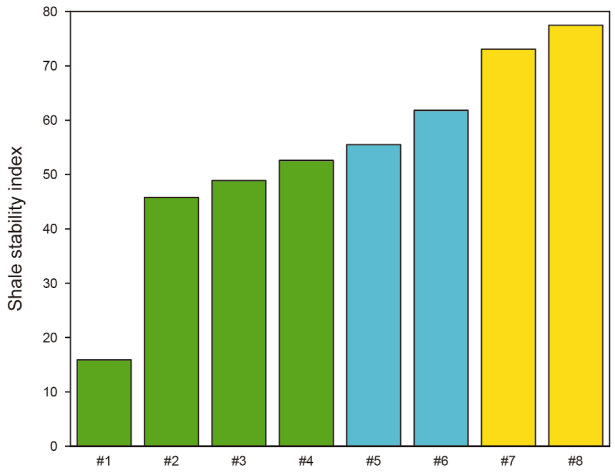

Fig. 9. SSI values for rock samples following immersion in different solutions.

3.2.4. Plugging agent optimization

Enhancing the plugging of formation fractures by drilling fluids is crucial for impeding the transmission of drilling fluid pressure and the invasion of filtrate, which is essential for maintaining wellbore stability (Tchameni et al., 2024; Du et al., 2025). Using a base fluid consisting of "2% bentonite slurry + 0.15% polymer viscosifier (HXC) + 2% poly (alkenyl sulfonate) fluid loss reducer (PAS)", various types of plugging agents named YFT, FFT, SN, and DFT were added at a concentration of 2.5%. Following 16 h of hot rolling at 150 °C, the API (American Petroleum Institute) filtrate loss (FL_{API}), the high-temperature and high-pressure (HTHP) filtrate loss (FL_{HTHP}) under conditions of 150 °C and 3.5 MPa, along with the rheological parameters of the experimental slurry, including the apparent viscosity (AV), plastic viscosity (PV), and yield point (YP), were evaluated (Huang et al., 2021b; Yang et al., 2024a). The experimental results are presented in Table 6. Triplicate testing was performed for drilling fluid rheology, fluid loss, and pH measurements, with results reported as mean values. The Bingham plastic model was employed to determine the rheological properties of the drilling fluid. The data indicate that, among the four types of plugging agents tested, the asphalt-based plugging agent named FFT exhibited the lowest filtrate volume, measuring 21 mL. Its plugging effect under high-temperature and high-pressure conditions was significantly superior to that of the other three plugging agents, and it also yielded the thinnest filter cake, thereby mitigating the formation of a falsely thick filter cake. Furthermore, among the four plugging agents, FFT also exhibited the lowest API filtrate loss and the thinnest filter cake. In addition, the experimental slurry incorporating FFT did not exhibit significant thickening, indicating that FFT possesses favorable compatibility with the drilling fluid base slurry used on-site and does not induce substantial adverse effects on the rheological properties of

Table 6
Optimization results for plugging agents.

Plugging agent	AV, mPa·s	PV, mPa·s	YP, Pa	FL_{API}, mL	FL_{HTHP}, mL	pH
YFT	52.5	35.0	17.5	6.6	36.0	8.5
FFT	41.0	29.0	12.0	6.2	21.0	9
SN	42.5	31.0	11.5	6.0	30.0	8.5
DFT	34.0	24.0	10.0	6.6	26.0	8.5

the drilling fluid. Therefore, considering both the plugging performance and the rheological properties, FFT was selected as the optimal plugging agent for the drilling fluid.

3.2.5. Drilling fluid formulation optimization

Based on the shale inhibitors, encapsulator, and plugging agent selection detailed above, the WBDF formulation used on-site was optimized considering the rheological property, filtration property, wellbore stabilizing property, and lubricity. The resulting formulation is as follows: 2% bentonite + 0.08% viscosifier HXC + 0.3% encapsulator BYJ + 1.2% fluid loss reducer PAS + 2% plugging agent FFT + 2.5% polyglycol lubricant YRH + 3% KCl + 1% polyamine + barite (weighting agent). All the additives were provided by PetroChina Dagang Oilfield Company.

3.3. Drilling fluid performance evaluation

In accordance with the density requirements for drilling fluids used in the Sha-1 and Sha-2 members within the target block, the rheological properties (Peng et al., 2024), filtrate loss (Tchameni et al., 2024; Zhao et al., 2024), and extreme pressure lubrication coefficient (Zhou et al., 2023; Yang et al., 2024b) of the optimized WBDF were evaluated both before and after 16 h of hot rolling at 150 °C, at densities of 1.3 and 1.4 g/cm^3, respectively. The results are presented in Table 7, where BR and AR denote “before hot rolling” and “after hot rolling”, respectively. Based on the measurements from a six-speed rotational viscometer, the Herschel-Bulkley model demonstrated the highest fitting accuracy for the rheological parameters of drilling fluids, while the Bingham model also achieved a correlation coefficient above 0.97, indicating its capability to accurately characterize the fluid’s rheological properties. Considering both the operational convenience and general acceptance in field applications, the Bingham model was adopted to calculate key rheological parameters, including AV, PV, YP, 10-s and 10-min gel strength of the drilling fluid. The data indicate that, under both density conditions, the optimized WBDF maintains favorable rheological properties, characterized by moderate viscosity and shear stress. Following 150 °C hot rolling, the ratio of yield point to plastic viscosity is maintained at approximately 0.4, ensuring adequate hole cleaning performance. The API filtrate loss after hot rolling remains within 5 mL, and the filtrate volumes under conditions of 150 °C and 3.5 MPa are 14 and 15.4 mL, respectively, demonstrating desirable filtration control properties. The extreme pressure lubrication coefficients of the drilling fluid under various conditions are approximately 0.1, indicating satisfactory lubrication performance.

To validate the wellbore-stabilizing performance of the optimized WBDF, shale samples from the Sha-1 Member were selected. The performance of the optimized WBDF (density of 1.3 g/cm^3) was compared to that of the previously utilized drilling fluid containing 7% KCl using both cuttings recovery rate and SSI experiments. The results indicate that the cuttings recovery rate in the previously utilized drilling fluid was 83.8%, with a corresponding SSI of 81.2. In contrast, the optimized WBDF exhibited a recovery rate of 87.9% and an SSI of 84.9, demonstrating favorable wellbore-stabilizing performance surpassing that of the previously utilized drilling fluid. These findings suggest that the combination of 3% KCl and 1% polyamine, serving as the shale inhibitor, provides inhibition performance equivalent to, or marginally better than, that of 7% KCl, thereby achieving the objective of effectively maintaining wellbore-stabilizing performance while simultaneously reducing the KCl concentration to ensure logging accuracy.

3.4. Field application

In 2023, the findings of this study were implemented in the Dagang Oilfield to optimize the WBDF with a low KCl concentration. The drilling operations for over ten exploration/appraisal wells were successfully completed in the CX block. The salinity of the drilling fluid was effectively controlled, and the logging interpretation consistency rate improved from 68.1% to 89.9% compared to historical data from before 2022. Throughout the operations, wellbore stability was maintained, resolving the previous challenge in this block of balancing wellbore stability and logging interpretation accuracy in exploration/appraisal well operations. Taking the CX-1 exploration/appraisal well as a representative example, the KCl concentration of the drilling fluid was adjusted during field operations from the originally designed 6%–7% to 3%–4%, and the drilling fluid resistivity at room temperature was adjusted from 0.1 to 0.22 Ω·m. This adjustment facilitated the establishment of a precise logging interpretation profile, enabling accurate evaluation of the oil, gas, and water-bearing zones. This, in turn, laid the foundation for achieving a daily production of up to 100 tons of crude oil in the Sha-2 Member reservoir during oil testing in this well. Moreover, the wellbore diameter remained consistent throughout the operation, and no downhole complications, such as wellbore collapse or stuck pipe, were encountered. The mechanical drilling rate also improved by 8% compared to the neighboring block completed in 2022.

In 2024, this success was further extended and applied to the drilling fluid design and implementation in regions such as the Cangdong and Qikou deep sag areas. This expansion resulted in a further improvement in the logging interpretation consistency rate, leading to enhanced evaluation and interpretation outcomes for self-sourced and self-sealing reservoirs. Within the Cangdong block, the interpreted oil layer thickness increased, and a greater proportion of wells exhibited high production rates following perforation. Concurrently, the exceptional inhibition and wellbore-stabilizing properties of the drilling fluid ensured wellbore stability, and fewer downhole complications arising from wellbore instability were observed. The incidence of wellbore collapse and drill pipe sticking was reduced by 90 % compared to 2023. This contributed technical support for the high-quality completion of drilling operations and accurate reservoir evaluation in exploration/appraisal wells.

Table 7
Experimental results of drilling fluid performance evaluation.

Density, g·cm^{-3}	Condition	AV, mPa·s	PV, mPa·s	YP, Pa	Gel strength, Pa		FL_{API}, mL	FL_{HTHP}, mL	pH	Lubrication coefficient
					10 s	10 min				
1.3	BR	60.5	40	20.5	11	22	4.1		9	0.0913
	AR	50.5	36	14.5	5	8	3.4	14.0	9	0.0961
1.4	BR	72.5	49	23.5	14	24	3.9		9	0.0958
	AR	56	40	16	5	9	4.4	15.4	9	0.1013

4. Conclusions

(1) An analytical model was developed to evaluate the influence of KCl concentration in drilling fluids on the accuracy of array induction logging responses. The model's calculations indicate that, under consistent formation resistivity conditions, as the drilling fluid resistivity increases, the influence of drilling fluid resistivity on the logging response diminishes, and the curves progressively converge, approaching the true formation resistivity. Consequently, the critical drilling fluid resistivity threshold required to ensure logging accuracy is governed by the formation resistivity. As the KCl concentration in the drilling fluid increases, the resistivity decreases, and the accuracy of the logging response curve declines. For the target block in the Dagang Oilfield, specifically the Dong-3 Member, maintaining the KCl concentration in the drilling fluid at $\leq$ 4.8% ensures a logging accuracy of no less than 80% across all layers. For the Sha-1 Member, the KCl concentration in the drilling fluid should be $\leq$ 4.2%, while for the Sha-2 Member, the KCl concentration should be $\leq$ 3.6% to meet the accuracy requirements.

(2) As the KCl concentration increases, the shale cuttings recovery rate gradually increases. However, when the concentration exceeds 3%, the rate of increase in recovery diminishes. Therefore, to ensure effective shale inhibition, the KCl concentration should be maintained at a minimum of 3%. The cuttings recovery rate achieved with 3% KCl combined with polyamine at a concentration of at least 1% is close to or reaches that achieved with 7% KCl. Moreover, the shale stability index is marginally higher than that of 7% KCl, indicating that the synergistic inhibition performance of the combination is excellent. This combination can effectively replace 7% KCl and is the preferred shale inhibitor combination for low-concentration KCl drilling fluids. Furthermore, the incorporation of a polymer encapsulator can effectively mitigate the hydration of shales within the target formation.

(3) Based on the WBDF formulation utilized in the field, an efficient WBDF with low KCl concentration was optimized. This optimized fluid exhibits good rheological, filtration, and lubricity properties, along with excellent wellbore-stabilizing performance. This drilling fluid has been applied in exploration/appraisal wells across multiple blocks within the Dagang Oilfield. This application resulted in an improvement in the consistency of electric logging interpretation from 68.1% before 2022 to 89.9%. Additionally, the wellbore stability during operations was maintained, addressing the previous challenge in exploration/appraisal wells within this block, where balancing wellbore stability and logging interpretation accuracy proved difficult. This, in turn, has provided technical support for the high-quality completion of drilling operations and precise reservoir evaluation in exploration/appraisal wells.

CRediT authorship contribution statement

Xin Zhao: Writing – original draft, Project administration, Methodology, Investigation. **Ying-Bo Wang:** Visualization, Validation, Resources. **Fu-Hua Cao:** Software, Investigation, Data curation. **Cao-Yuan Niu:** Writing – review & editing, Data curation. **Zi-Qing Liu:** Methodology. **Lei Wang:** Supervision, Methodology, Formal analysis.

Declaration of competing interest

The authors declare that they have no known competing financial interests or personal relationships that could have appeared to influence the work reported in this paper.

Acknowledgments

This work was supported by the National Natural Science Foundation of China (52474024), the National Oil & Gas Major Project of China (2025ZD1403200), and the Program for Scientific Research Innovation Team of Young Scholars in Colleges and Universities of Shandong Province "Innovation Team of Deepwater Wellbore Fluids" (2022KJ069).

Nomenclature

AV	apparent viscosity, mPa·s
D	average swelling height or erosion depth of the rock sample after soaking, mm
FL_{API}	API fluid loss, mL
FL_{HTHP}	high-temperature and high-pressure fluid loss, mL
H_f	penetration value of the rock sample after soaking, mm
H_i	penetration value of the rock sample prior to soaking, mm
PV	plastic viscosity, mPa·s
YP	yield point, Pa

Abbreviations

API	American Petroleum Institute
AR	after hot rolling
BR	before hot rolling
BYJ	acrylamide-based polymer encapsulator
FFT	asphalt-based plugging agent
HDIL	high definition induction logging
HTHP	high-temperature and high-pressure
HXC	polymer viscosifier
I/S	illite/smectite
NMR	nuclear magnetic resonance
PAS	poly (alkenyl sulfonate) fluid loss reducer
SSI	shale stability index
WBDF	water-based drilling fluid
YRH	polyglycol lubricant

References

Baggieri, R.R., Carrasquilla, A.A.G., Ceia, M.A.R., et al., 2024. Impacts of a new drilling fluid invasion on electrical resistivity and acoustic velocity measurements. Energy Fuel. 38 (5), 4752–4768. https://doi.org/10.1021/acs.energyfuels.3c01949.

Doughty, C., Tsang, C.F., Rosberg, J.E., et al., 2017. Flowing fluid electrical conductivity logging of a deep borehole during and following drilling: estimation of transmissivity, water salinity and hydraulic head of conductive zones. Hydrogeol. J. 25 (2), 501–517. https://doi.org/10.1007/s10040-016-1497-5.

Du, H.Y., Lv, K.H., Sun, J.S., et al., 2025. Mesoporous SiO_2 nanoparticles with low surface energy and multi-level roughness as shale wellbore stabilizers in oil-based drilling fluid. Pet. Sci. 22 (1), 384–397. https://doi.org/10.1016/j.petsci.2024.12.006.

Huang, D.C., Xie, G., Peng, N.Y., et al., 2021a. Synergistic inhibition of polyethylene glycol and potassium chloride in water-based drilling fluids. Pet. Sci. 18 (3), 827–838. https://doi.org/10.1007/s12182-020-00543-w.

Huang, W.A., Wang, J.W., Lei, M., et al., 2021b. Investigation of regulating rheological properties of water-based drilling fluids by ultrasound. Pet. Sci. 18 (6), 1698–1708. https://doi.org/10.1016/j.petsci.2021.09.006.

Jiang, Y.J., Zhou, J., Fu, X.F., et al., 2021. Analyzing the origin of low resistivity in gas-bearing tight sandstone reservoir. Geofluids (1), 4341804. https://doi.org/10.1155/2021/4341804.

Kozlowski, M., Chakraborty, D., Jambunathan, V., et al., 2021. An integrated petrophysical workflow for fluid characterization and contacts iidentification using NMR continuous and stationary measurements in a high-porosity

sandstone formation, offshore Norway. Petrophysics 62 (2), 210–226. https://doi.org/10.30632/PJV62N2-2021a5.
Li, H., Liu, D.R., Ni, X.W., et al., 2019. Logging responses of electromagnetic wave resistivity while drilling with drilling fluid intrusion. Fault-Block Oil Gas Field 26 (5), 675–680. https://doi.org/10.6056/dkyqt201905028 (in Chinese).
Li, H., Huang, X.B., Sun, J.S., et al., 2023. Improving the anti-collapse performance of water-based drilling fluids of Xinjiang oilfield using hydrophobically modified silica nanoparticles with cationic surfactants. Pet. Sci. 20 (3), 1768–1778. https://doi.org/10.1016/j.petsci.2022.10.023.
Liu, R.M., Zhang, W.X., Chen, W.X., et al., 2025. Factors and detection capability of look-ahead logging while drilling (LWD) tools. Pet. Sci. 22 (2), 850–867. https://doi.org/10.1016/j.petsci.2024.12.024.
Lu, J., Wang, B., Ji, H., et al., 2017. A Novel Lateral Resistivity logging-while-drilling (LWD) Method in Oil-based Drilling Fluid. Chinese Automation Congress (CAC), pp. 1245–1249. https://doi.org/10.1109/CAC.2017.8242957.
Mondshine, T.C., 1973. A New Potassium Based Mud System. Fall Meeting of the Society of Petroleum Engineers of AIME. https://doi.org/10.2118/4516-ms.
Murtaza, M., Gbadamosi, A., Hussain, S.M.S., et al., 2023. Experimental investigation of pyrrolidinium-based ionic liquid as shale swelling inhibitor for water-based drilling fluids. Geoenergy Sci. Eng. 231, 212374. https://doi.org/10.1016/j.geoen.2023.212374.
Peng, J.H., Zhang, H.H., Li, X.L., et al., 2024. Effect of concentration and functional group of cellulose nanocrystals on the rheological and filtration properties of water-based drilling fluids at various temperatures. Cellulose 31 (8), 5151–5169. https://doi.org/10.1007/s10570-024-05890-0.
Ramadan, A.M., Osman, A., Mehanna, A., et al., 2024. Simulation of filter-cake formations on vertical and inclined wells under elevated temperature and pressure. SPE J. 29 (5), 2212–2224. https://doi.org/10.2118/219446-pa.
Rasouli, F.S., 2022. Does mudcake change the results of modeling gamma-gamma well-logging? Nucl. Eng. Technol. 54 (9), 3390–3397. https://doi.org/10.1016/j.net.2022.03.028.
Shi, X.C., Wang, L., Guo, J.H., et al., 2019. Effects of inhibitor KCl on shale expansibility and mechanical properties. Petroleum 5 (4), 407–412. https://doi.org/10.1016/j.petlm.2018.12.005.
Sukhorukova, K.V., Petrov, A.M., Lapkovskaya, A.A., et al., 2025. Methodological aspects of electrical logging data integration for inversion based on two-dimensional axisymmetric formation models. Russ. Geol. Geophys. 66 (4), 471–480. https://doi.org/10.2113/rgg20244813.
Sun, J.S., Wang, Z.L., Liu, J.P., et al., 2022. Notoginsenoside as an environmentally friendly shale inhibitor in water-based drilling fluid. Pet. Sci. 19 (2), 608–618. https://doi.org/10.1016/j.petsci.2021.11.017.
Tchameni, A.P., Zhuo, L.Y., Wandji Djouonkep, L.D., et al., 2024. A novel responsive stabilizing Janus nanosilica as a nanoplugging agent in water-based drilling fluids for exploiting hostile shale environments. Pet. Sci. 21 (2), 1190–1210. https://doi.org/10.1016/j.petsci.2023.10.008.
Wang, S., Xie, R.H., Jin, G.W., et al., 2024. A new method for fluid identification and saturation calculation of low contrast tight sandstone reservoir. Pet. Sci. 21 (5), 3189–3201. https://doi.org/10.1016/j.petsci.2024.07.005.
Xie, G., Fu, L., Gu, S., et al., 2024. Investigation on the interlayer intercalation inhibition mechanism of polyamines with different adsorption functional groups on montmorillonite: experiment and density functional theory simulation. Geoenergy Sci. Eng. 233, 212532. https://doi.org/10.1016/j.geoen.2023.212532.
Xiong, W.J., Xiao, L.Z., Yuan, J.R., et al., 2024. Automatic depth matching method of well log based on deep reinforcement learning. Petrol. Explor. Dev. 51 (3), 634–646. https://doi.org/10.11698/PED.20230460.
Xu, C.C., Torres-Verdín, C., Gao, R., 2013. Interpretation of hydraulic rock types with resistivity logs in tertiary deepwater turbidite reservoirs: pore-scale modeling verified with field observations in the Gulf of Mexico, USA. Interpretation 1, T177–T185. https://doi.org/10.1190/INT-2013-0037.1.
Yang, F., Cheng, C., Qiu, J.M., et al., 2023. Research progress on corkscrew borehole logging curve correction method. Well Logging Technol. 47 (4), 398–405. https://doi.org/10.16489/j.issn.1004-1338.2023.04.002 (in Chinese).
Yang, J., Jiang, G.C., Yi, J.T., et al., 2024a. Natural rubber latex as a potential additive for water-based drilling fluids. Pet. Sci. 21 (4), 2677–2687. https://doi.org/10.1016/j.petsci.2024.04.012.
Yang, L.L., Liu, Z.Y., Wang, S.B., et al., 2024b. Chemical modification of barite for improving the performance of weighting materials for water-based drilling fluids. Pet. Sci. 21 (1), 551–566. https://doi.org/10.1016/j.petsci.2023.10.001.
Zhang, S.F., Wang, H.G., Qiu, Z.S., et al., 2019. Calculation of safe drilling mud density window for shale formation by considering chemo-poro-mechanical coupling effect. Petrol. Explor. Dev. 46 (6), 1271–1280. https://doi.org/10.11698/PED.2019.06.17.
Zhao, A.S., He, X., Chen, H., et al., 2023. Response analyses on the drill-string channel for logging while drilling telemetry. Pet. Sci. 20 (5), 2796–2808. https://doi.org/10.1016/j.petsci.2023.03.007.
Zhao, X., Zhang, H., Wang, S., et al., 2024. Characterization and performance evaluation of modified apatite ore as a new scid-soluble weighting agent for drilling fluids. SPE J. 29 (1), 55–63. https://doi.org/10.2118/217473-PA.
Zheng, X.B., Hu, H.S., Guan, W., et al., 2014. Theoretical simulation of the electric field induced by acoustic waves during the seismoelectric logging while drilling. Chin. J. Geophys. 57 (1), 320–330. https://doi.org/10.6038/cjg20140128.
Zhong, H.Y., Qiu, Z.S., Huang, W.A., et al., 2011. Shale inhibitive properties of polyether diamine in water-based drilling fluid. J. Pet. Sci. Eng. 78 (2), 510–515. https://doi.org/10.1016/j.petrol.2011.06.003.
Zhou, S.S., Song, J.J., Xu, P., et al., 2023. A review on tribology, characterization and lubricants for water-based drilling fluids. Geoenergy Sci. Eng. 229, 212074. https://doi.org/10.1016/j.geoen.2023.212074.